hole collisions[17] provide sufficient scattering to limit the mobility to the observed values at high temperatures and may be the dominant mechanism there. Using the estimate of E_1 previously given and the thermal expansion coefficient $\alpha = 14.4 \times 10^{-6}$ deg^{-1} of Mokrowski and Regel,[18] the change of activation energy with temperature due to thermal expansion of the lattice can be calculated. It is 1.0×10^{-4} ev/deg, which is to be compared with the value 2.6×10^{-4} ev/deg derived from the shift of the infrared absorption edge by Austin and McClymont.[2] Even allowing for possible error in the compressibility, a considerable portion of the temperature variation of the gap must be attributed to direct electron-phonon interactions.

[17] F. J. Morin and J. P. Maita, Phys. Rev. **94**, 1525 (1954).
[18] H. P. Mokrowski and A. R. Regel, J. Tech. Phys. (U.S.S.R.) **22**, 1281 (1952).

8. ACKNOWLEDGMENTS

The author is indebted to the Chicago Midway Laboratories and Dr. S. W. Kurnick for the InSb used in this experiment and to Dr. C. Kittel and co-workers at the University of California for communication of their cyclotron resonance results prior to publication. He also wishes to thank Dr. E. N. Adams, Dr. R. L. Longini, and Dr. F. Keffer for critical reviews of the manuscript.

PHYSICAL REVIEW VOLUME 99, NUMBER 2 JULY 15, 1955

Distribution of Electrons Scattered by Gold*

L. MARTON, J. AROL SIMPSON AND T. F. MCCRAW
National Bureau of Standards, Washington, D. C.
(Received April 14, 1955)

The distribution in energy and angle of 20-kev electrons scattered by gold has been measured. The energy resolution is better than 0.1 percent and the angular resolution better than 10^{-3} radian. Data are presented for gold of different thickness and degree of crystal orientation and for grazing angle reflection.

ALTHOUGH the interactions of electrons with matter have been extensively studied in the past, most of the interest has been directed either to incident energies so high that the most important contribution to the scattering is nuclear, or to energies of at most a few hundred electron volts where secondary emission is of primary interest. With a few notable exceptions,[1] the range of energies from a few kev to one hundred kev has until recently been neglected. Yet this region of the energy spectrum can give information on the imaginary part of the complex dielectric constant used in the semi-classical theory of stopping power, or from another point of view, information on the density effects on the elementary interactions processes. This knowledge is of interest both to the solid state and radiation physics. Interest in this region was revived in Germany just after the war when Mollenstedt[2] with the aid of an improved electrostatic analyzer, began to study the energy losses of electrons in the forward direction (0–10^{-3} rad). This work was extended by the studies of Marton and Leder[3] in America and workers in Japan and Germany.[4] The interest was centered on the characteristic losses of the scatterers which are more or less discrete losses ranging from 1 to 100 electron volts. With a modified Mollenstedt apparatus Leonhard[5] and Watanabe[6] have extended these measurements to include the distribution in angle. The electrostatic analyzer when used in this manner is somewhat unsatisfactory, being nonlinear in energy and intensity and having a poorly defined acceptance angle.

To overcome these limitations we have constructed an apparatus using a double-focusing magnetic analyzer and the geometry shown in Fig. 1. This instrument, which will be described in detail elsewhere, is automatic in operation and gives a record of the energy spectrum of the scattered electrons with an energy resolution of better than 0.1 percent at angular intervals of less than 10^{-3} radian over a range of 300 degrees. The relative value

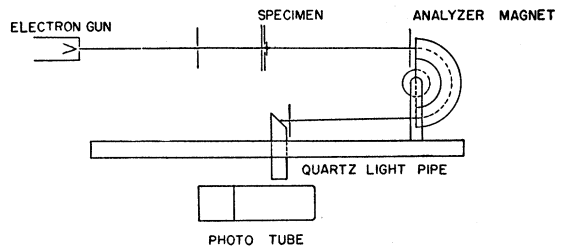

FIG. 1. Electron trajectory showing relative placement of principal elements of the scattering instrument.

* This work was in part supported by the Office of Naval Research.
[1] G. Ruthemann, Naturwiss. **29**, 648 (1941); Ann. Physik (6) **2**, 113 (1948); W. Lang, Optik **3**, 233 (1948).
[2] G. Mollenstedt, Optik **5**, 499 (1949); **9**, 473 (1952).
[3] L. Marton and L. B. Leder, Phys. Rev. **94**, 203 (1954); L. B. Leder and L. Marton, Phys. Rev. **95**, 1345 (1954).
[4] H. Watanabe, J. Phys. Soc. Japan **9**, 920 (1954); **9**, 1035 (1954); Phys. Rev. **95**, 1684 (1954); W. Klein, Optik **11**, 226 (1954).
[5] F. Leonhard, Z. Naturforsch. **99**, 727 (1954).
[6] H. Watanabe (private communication).

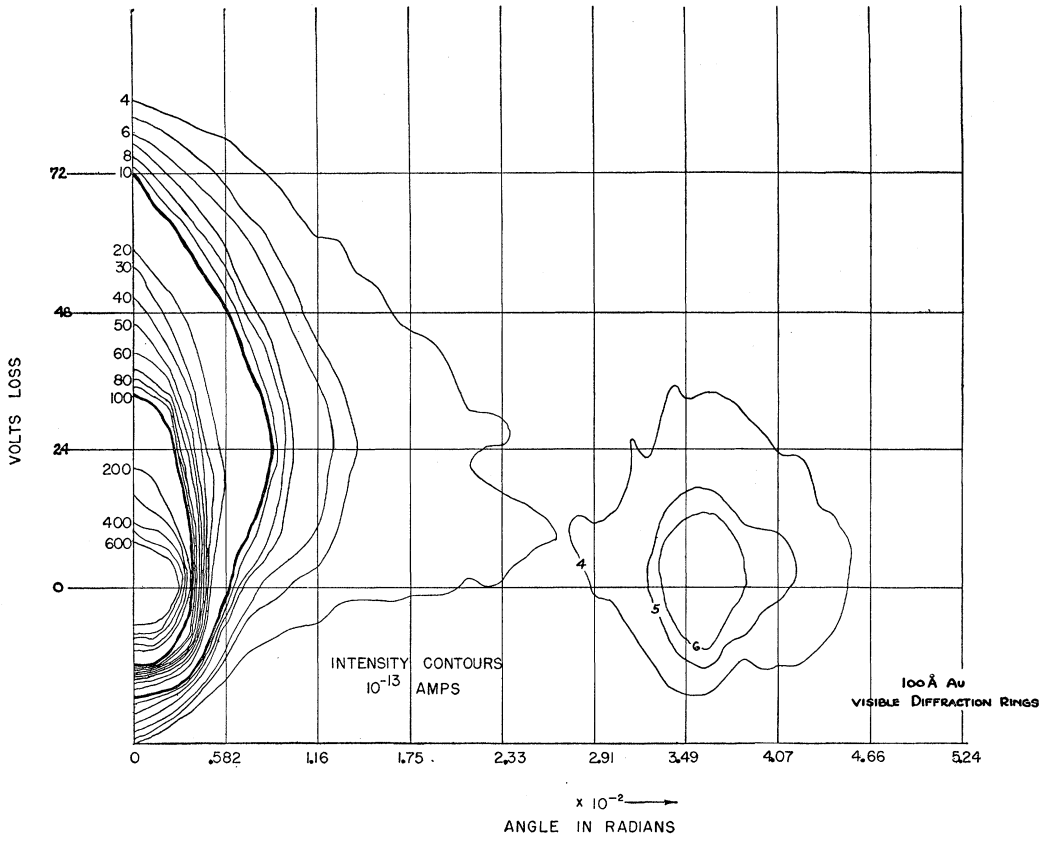

FIG. 2. Cartographic plot of the distribution of 20-kev electrons scattered by 100 A polycrystalline gold. The abscissa is angle, the ordinate energy loss in ev, and the contours of equal intensity, in 10^{-13} ampere.

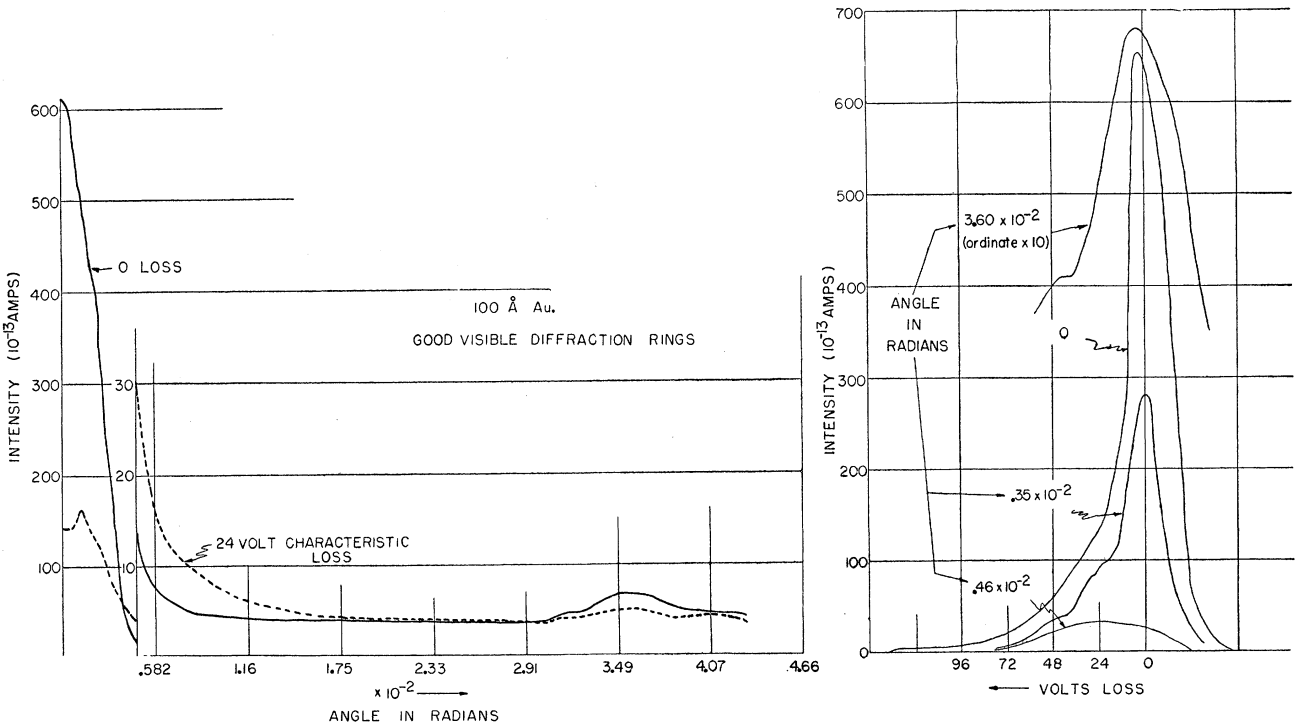

FIG. 3. Left: Graph of scattered intensity as a function of angle. Both elastic and 24-ev characteristic energy loss curves are shown. Right: Graph of scattered intensity as a function of energy loss in ev at selected angles. Polycrystalline 100 A gold, 20-kev incident energy.

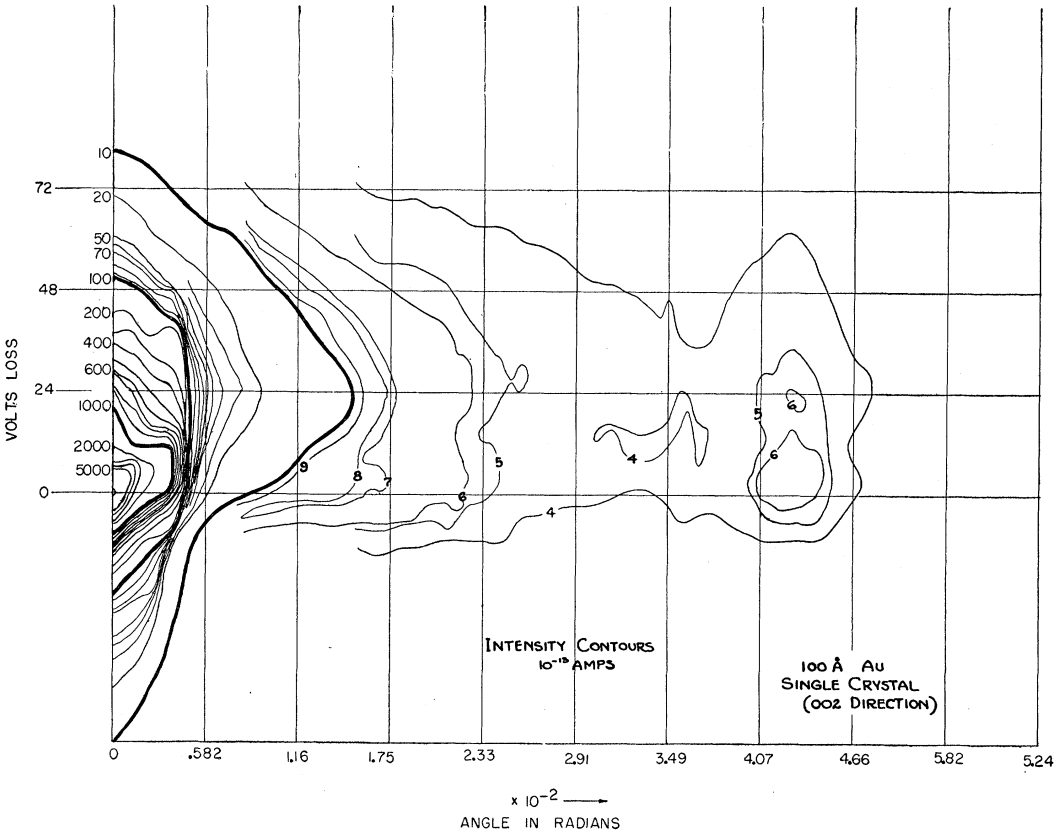

FIG. 4. Cartographic plot of the distribution of 20-kev electrons scattered by 100 A single crystal gold. The abscissa is angle, the ordinate energy loss in ev, and the contours of equal intensity in 10^{-13} ampere.

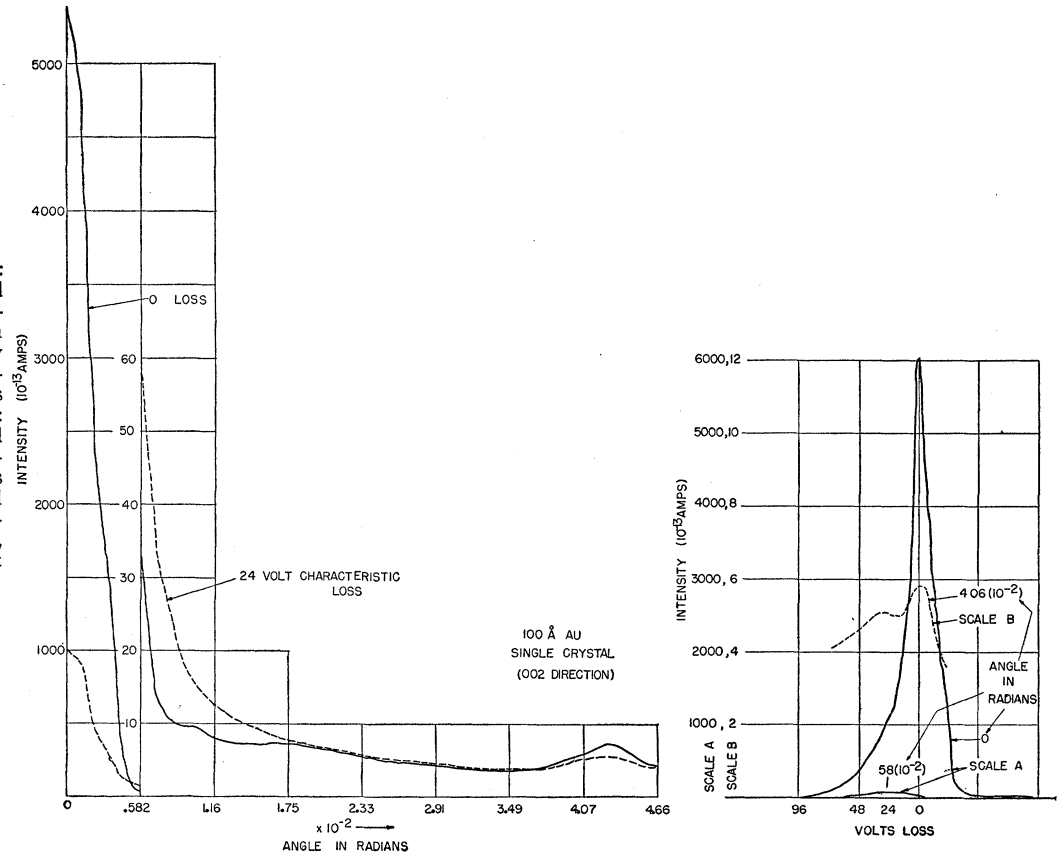

FIG. 5. Left: Graph of scattered intensity as a function of angle. Both elastic and 24-ev characteristic energy loss curves are shown. Right: Graph of scattered intensity as a function of energy loss in ev at selected angles. Single crystal 10 A0 gold, 20-kev incident energy.

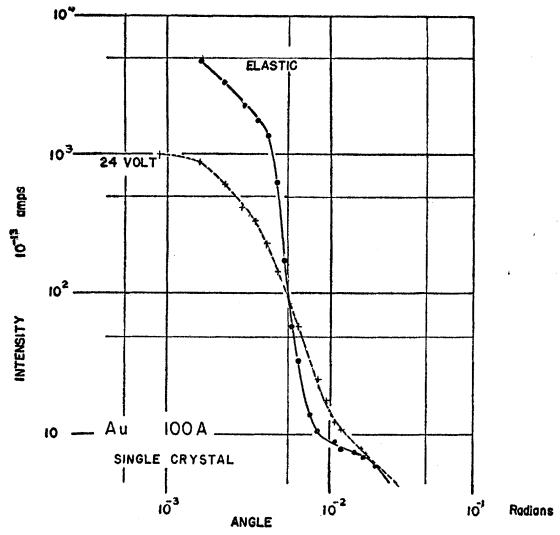

FIG. 6. Data from Fig. 5, left, replotted on log-log scale.

of the energy loss is more precise than the absolute values, for which the error in calibration may be as large as 5 percent of the loss.

The results of a study of scattering of 20-kev electrons by Au is presented in Figs. 2–6. The films of spectrochemically pure gold, which were of different thickness and degree of orientation, were prepared by vacuum evaporation. The degree of orientation in the polycrystalline samples was controlled by rate of evaporation, slow evaporation giving larger crystallites than rapid evaporation. To prepare single crystals, the gold was evaporated upon a rock salt substrate which was heated to 400°C. Under these conditions good single crystals are produced by epitaxy. Figure 2 is a cartographic presentation of the scattering from a polycrystalline gold foil of 100 A thickness. The X coordinate is angle, Y is energy loss, and Z is intensity which is represented by lines of equal value. Because of the range of intensities covered, these contours are given on a logarithmic scale. This logarithmic scale must be considered if the cartographs are read as contour maps, since the low levels are emphasized. It is

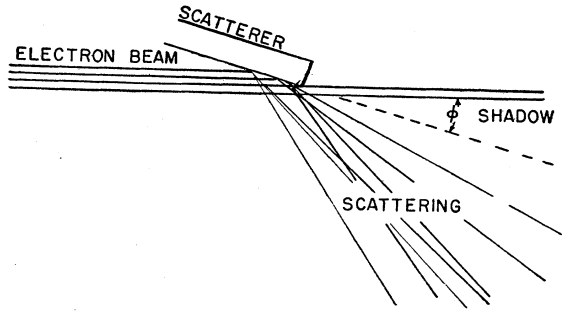

FIG. 7. Sketch of the geometry used to obtain scattering pattern shown in Fig. 8. The source of the zero angle and scattered maxima are shown.

this fact that makes the portion below the zero axis, which is due to finite line widths and phosphor decay time, appear so prominent. A less distorted view of the energy profile can be seen on the right of Fig. 3. This figure shows that the intensity distribution on a linear scale is a function of energy at selected angles. To the left of Fig. 3 is plotted the intensity as a function of angle at the fixed energy losses of zero ev and 24 ev. It is interesting that from an initially higher value the zero-loss line falls below the characteristic loss at an angle of 20 minutes and continues below until it rises more rapidly and recrosses the loss line at the first diffraction maximum. The fact that the loss line also rises lends support to the suggestion of Farnsworth[7] that the scattering is a two-step process with the loss occurring before or after the diffraction. The long flat region between the initial fall-off and the first diffraction suggests that a screened Coulomb interaction plays a major role.

Figures 4 and 5 present similar data for a gold single crystal of 100-A thickness. The scattering pattern is similar to that just discussed. Figure 6 shows the fall-off of the center maximum plotted on a log log scale. It is obvious that no simple power law is obeyed; the linear portion of the zero-loss curve falls as the sixth power while the characteristic loss falls as the third power of the angle.

TABLE I. Comparison of some scattering characteristics for different degrees of crystal orientation and thickness of gold. I_{el} is the elastic scattering intensity, I_{ch} the characteristic energy loss intensity, and θ the angular position at which $I_{el}/I_{ch}=1$.

Gold film	I_{el}/I_{ch} at zero degrees	θ ($\times 10^{-3}$ radian) at $I_{el}/I_{ch}=1$
100 A single crystal	6	4.9
100 A large crystallite	4	3.9
100 A small crystallite	5	5.5
200 A small crystallite	3.6	4.4
400 A small crystallite	2.9	3.1

Table I gives a summary of the most prominent effects of varying the thickness and degree of crystalline orientation (crystallite size) of the scattering foil. The first column gives the degree of crystalline orientation (crystallite size) judged by the visibility of the diffraction pattern, the second the ratio of the elastic to characteristic loss at zero angle, and the third the smallest angle at which the cross sections are of equal value. It will be noted that as the thickness increases the relative value of the loss peak increases while the cross over is moved to lower angles. The effect of crystalline orientation is less clear-cut.

The geometry used to study Au at almost grazing incidence is sketched in Fig. 7. In this case the specimen was a thick (>1 micron) polycrystalline film deposited on fire polished glass. In the cartograph of Fig. 8, the

[7] J. C. Turnbull and H. E. Farnsworth, Phys. Rev. **54**, 509 (1938).

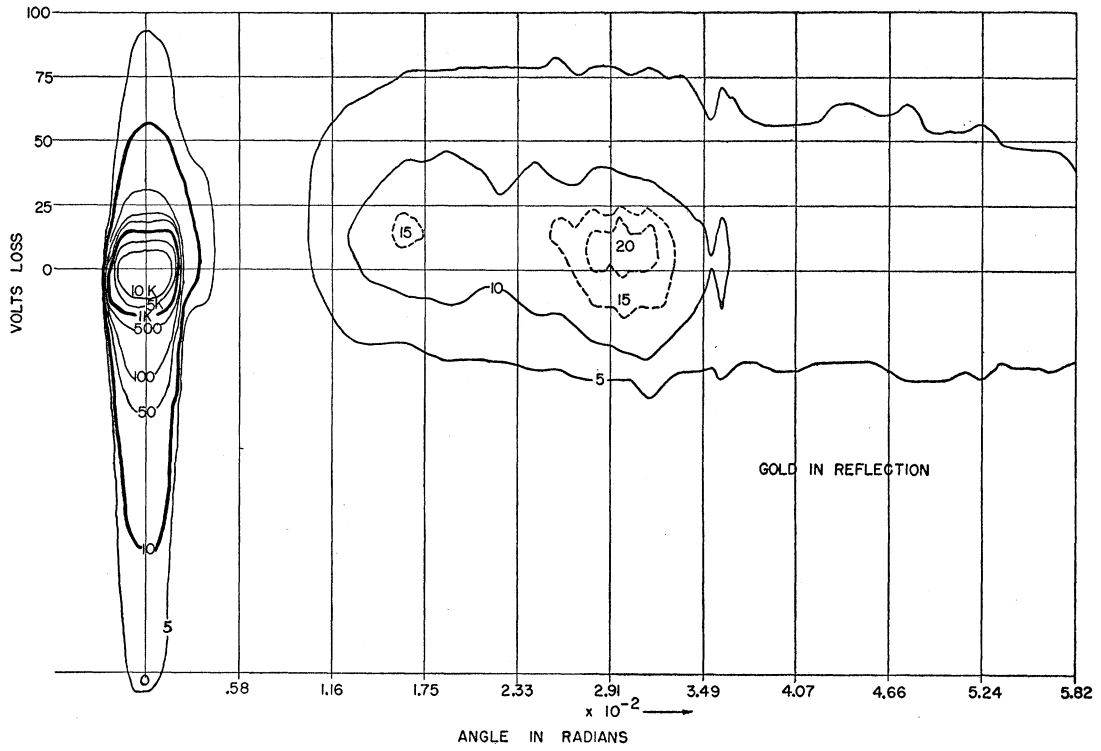

FIG. 8. Cartographic plot of reflection of 20-kev electrons by gold. Note lack of marked specular reflection and wide energy spread of scattered beam. The extreme extension of the contours at zero angle to regions above the zero loss is a result of finite detector time constant and is not significant.

unscattered portion of the initial beam can be seen to the left followed by the region in the shadow of the sample and the region of reflection. It will be noted that even at less than 10^{-2} radian there is no clearly defined specular reflection. Neither of the two small maxima can be definitely identified. The most notable difference between this and the transmission samples is the much wider distribution of energy in the scattered beam. This broadening is to be expected since multiple events are now far more probable. The broadening in angular distribution is similarly explained.

These studies are being extended to other materials while efforts are being made to increase the energy resolution of the instrument.